Elemental quantification and radioactive characterization of soil from Douala Bassa area: littoral region of Cameroon using X- and *γ*-rays spectrometry

Environmental Research Communications

PAPER

Elemental quantification and radioactive characterization of soil from Douala Bassa area: littoral region of Cameroon using X- and γ-rays spectrometry

Joel Cebastien Shouop Guembou[1,2,3], **Maurice Moyo Ndontchueng**[3,4], **Jilbert Eric Mekongtso Nguelem**[2,3], **Gregoire Chene**[1], **Steve Kayo**[2], **Ousmanou Motapon**[4] **and David Strivay**[1]

[1] Atomic and Nuclear Spectroscopy, Archeometry, UR Art, Archéologie, Patrimoine, University of Liège, Bât. B15 Sart Tilman, 4000 Liège 1, Belgium
[2] Fundamental Physics Laboratory - Mathematics, Applied Computer Sciences, and Fundamental Physics, University of Douala P O Box: 24157 Douala, Cameroon
[3] National Radiation Protection Agency, P O Box 33732, Yaounde, Cameroon
[4] Department of Physics, Faculty of Sciences, University of Douala. P O Box 24157 Douala–Cameroon

E-mail: sebastianguembou@gmail.com

OPEN ACCESS

RECEIVED
31 December 2018

REVISED
20 March 2019

ACCEPTED FOR PUBLICATION
29 April 2019

PUBLISHED
28 June 2019

Keywords: elemental quantification, EDXRF, gamma-ray spectrometry, BEGe, Fe-soil, x-ray spectrometry, soil

Abstract

The objectives of the present work were to characterize the investigated soil using EDXRF and to evaluate the radioactivity concentration of the primordial radionuclides using gamma-ray spectrometry-based High Purity Germanium (HPGe) detector, Broad energy type (BEGe). Soil characterization using EDXRF in the present study gives an overview of the geological origin or provenience of the investigated area. As a result, the analyzed soil samples can be classified chemically as Fe-soil and are illustrative dregs from the Continental margin because of high concentration of Fe (its concentration ranged from 14.78% to 22.26%) in all the investigated samples. The plotting of Al_2O_3/SiO_2 (%) as a function of Fe_2O_3 and MgO (%) for the eighteen sample points investigated from Douala and the diagram for the tectonic discrimination of sediment provenance evidenced that all soil samples are residue from Passive margins. The observed activity concentration profile of the primordial radionuclides and the calculated radium equivalent activity show that no significant radiological risk can be observed for inhabitants within the study areas. As regards to that, the obtained results of the two analytical techniques could be viewed as baseline data for subsequent investigations on elemental characterization and radioactivity assessment in the study area.

1. Introduction

Recently, human technology has been improved and the interest in 'how the environment influence human being' is increasing nowadays. Human are interested in their exposure to natural gamma-emitting radionuclide as well the elemental composition of their environment since these factors can influence their understanding in preventing cancers (due to ionizing radiation), other health effects (due to ingestion of heavy metal in water through well exploration, …), weathering process that brings changes in their life. Many studies have been performed in view to characterize different samples and determine the risk related to the used or being involved in contact with such material (geological material, soil, sand, rock, water, air, foodstuff and other main components that are involved in human daily activity). The most useful methods being using nowadays are gamma spectrometry for gamma-ray emitters characterization and x-rays spectrometry for x-ray fluorescence characterization.

The Energy Dispersive x-ray Fluorescence well known as EDXRF method, is a useful nuclear technic for studying the elemental composition of soil sample in a large range of concentration, samples from different geological texture and matrices, inhomogeneous/homogeneous ones, and samples described as being formed with different mineral characterization and grain size as soil, sediments, sand and mineral as well as building material and ancient archaeological objects. Typical examples of these kinds of samples are soil or geological samples for which XRF elemental analysis is worldwide used. It is then a subject of importance to characterize

the environment where humans live and where many activities have been involved. The well-known x-ray spectrometry technique permits quick and precise simultaneous analysis of many elements in this view (Dziunikowski 1989, Agarwal 1991, Van Grieken and Markowicz 1993, Tsuji *et al* 2005, Brjesson and Mattsson 2007, Willis and Duncan 2008, Fittschen and Falkenberg 2011, Banas *et al* 2013).

Elemental and chemical characterization of geological samples, as well as soil's, is worthwhile in different scientific fields such as agriculture, geology, physics, biology or geography (Brjesson and Mattsson 2007, Fittschen and Falkenberg 2011, Banas *et al* 2013, Kubala-Kukus *et al* 2013). One of the main and generally used topics of these analyses is the impact on environmental contamination of soil in term of heavy metal's concentration, the provenience of different soil that may be highly radioactive and the relation between chemical composition and activity concentration. Information about the soil's elemental composition is also relevant to the knowledge of different processes as soil erosion and weathering, soil formation, its degradation and disintegration, its origin and provenience as well as in determining its geological till properties, useful for the advancement of applied science nowadays. It is thus necessary to bring a comparison between the composition, the structure and the morphology of different investigated samples and their origin and the reconstruction of their geo-history or source. The chemical composition of the sample is also relevant and must be considered in the quantitative description. Due to its non-homogeneity, it relies on morphological factors for is classification. The assessment of the different geochemical signatures, soil's quality, differentiating between the use of different type of land, soil's provenance and degradation are then functions of its physical and chemical properties (Glasby *et al* 2004, Hernández *et al* 2007, Franz *et al* 2013, Manso *et al* 2013, Melquiades *et al* 2013, Melquiades and Santos 2014 Walling 2013, Natara de Castilhos *et al* 2015, Stockmann *et al* 2016). XRF method is generally based on major, minor and trace elements' determination which composed geological materials. Environmental study assessments are then subjects of the determination of major element, minor's and trace's concentrations as well as radioactive concentration (Navas *et al* 2007). Many investigations are performed nowadays in different countries to access environmental radioactivity and associated radiological parameters.

The present study aims to analyze the soil samples from the coastal and most popular city in Cameroon, named Bassa –zone in the Littoral Region of Cameroon using the Energy Dispersive x-ray Fluorescence technic (Kheswa *et al* 2011, Kubala-Kukus *et al* 2013, Kubala-Kukus *et al* 2015, Baba *et al* 2016). In addition, radioactivity and radiological properties of analyzed samples were assessed for evaluating the exposure risk to the inhabitants of the studied area due to natural radiation.

To set gauges and national rules that are used for providing recommendations, it is always necessary to evaluate the radioactivity level on the national territory. For this reason, particular attention has been paying on the knowledge of radionuclide fixation in the soil in different nations and often worldwide (Beretka and Mathew 1985, Guembou *et al* 2017a). Radioactivity level was also determined using high purity germanium (HPGe) detectors based on gamma-ray spectrometry technic.

The interpretation with regards to the variation of the sample's matrix on the elemental characterization of the samples was done accordingly. The qualitative and quantitative improvement of the soil sample analysis was the main motivation of the undertaken research that had been done concerning the site characterization, a new and innovative subject in the region (Central Africa). It is a great interest in the research field since no data concerning this subject is available. The paper describes the experimental devices and measurement as well as the obtained results and discussion. The section conclusions summarize EDXRF and Gamma spectrometry studies of soil samples from the studied area.

2. Material and methods

2.1. Study area

The field of the experiment is a well-known region that covers the two campuses of the University of Douala—Cameroon, a site located within the basin of Douala, named 'Douala—Bassa' zone (04° 03′14.8″–04° 03′29.7″ N and 09° 44′00.1″–09° 44′45.2″ W). The geology of the site is characterized by sedimentary rocks from the tertiary to quaternary sediments as shown in figure 1 (Asaah Victor *et al* 2006). The formation of the investigated area consists dominantly of sandstones with a few intercalations of limestone and shale. The basin of Mungo consists of poorly consolidate grits and sandstones that used to be displayed bedding. Soils from the study area vary from yellow through brown to black ferralitic soils (Asaah Victor *et al* 2006). The details of the description of the study area are presented in research done by Guembou *et al* (2017b, 2016). It is a part of the largest city of Cameroon and Central Africa where the average annual temperature fluctuated around the value of 27.0 °C (80.6 °F). The studied area sits on high hydrology with flowing rivers as Wouri and Dibamba and characterized by a tropical climate. It typically features warm and humid conditions with an average annual humidity of ~83% and the rainfall is a particularity of the area which experiencing around 3600 millimeters (140 in) average of precipitation per year (World Weather Information Service WWIS 2016, Guembou *et al* 2017a, 2017b).

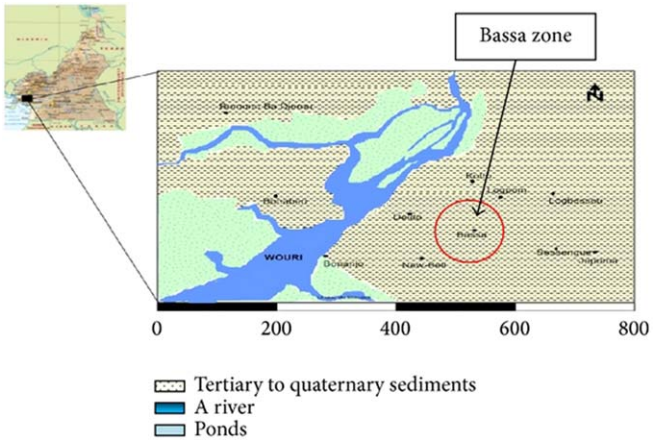

Figure 1. The study area: Douala Bassa area.

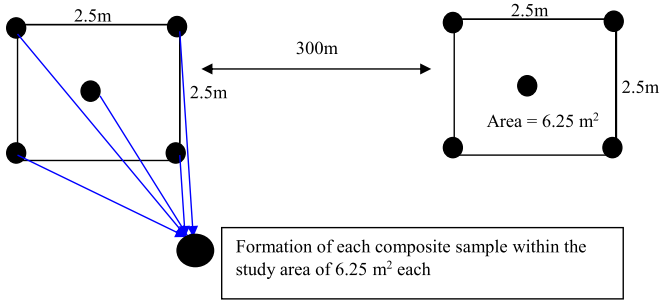

Figure 2. Composite sample collection within the sampling sites.

2.2. Sample collection and pellets preparation

Composites of 18 soil samples were randomly sampled from the 02 campuses, 07 from Campus 1 named ESSEC situated at Ange-Raphael and 11 from Campus 2 located at Ndong-Bong (Douala—Bassa area). For details concerning sampling method, the previously published research done by Guembou *et al* described the methodology used in the present research (Guembou *et al* 2017a, Guembou *et al* 2017b, Guembou *et al* 2016). The samples were labeled accordingly and transferred to the laboratory for specific preparation and analysis. Samples were dried at 60 °C for 48 h once in the lab, ground and sieved to achieve homogeneous content with a grain size less than 100 μm for XRF measurement. It was also dried at around 105 °C for 24 h in a special oven, a tool for gamma spectrometry, ground and sieved for grain size less than 250 μm for gamma spectrometry preparation (Guembou *et al* 2016). The sampling procedure is presented in Figure 2.

2.3. EDXRF experiment

2.3.1. Portable energy dispersive x-ray fluorescence spectrometer (EDXRF)

The Energy Dispersive x-ray Fluorescence (EDXRF) instrument used in this research is a powerful tool that can be very effective in the validation of both the absence and presence of certain elements in soil samples. This commercial instrument could be employed to provide rapid detection of the presence of elements such as Pb, Ni, As, Cr, Cd, Cu, Zn, and Hg in geological samples (Radu and Diamond 2009).

The portable XRF spectrometer used during acquisition consists of a MOXTEK instrument with an Rh x-ray tube (Ag target, 50 kV, and 5 W). The outcome radiations (x-rays) are collimated by a Ta ($Z = 73$) collimator bringing a 5 mm diameter beam at the sample surface. All the samples are placed at the same distance of 55 mm from the 10 mm from the SSD detector. The SSD (Super Silicon Drift) detector used for experiments is a 25 mm^2 detection area with 500 μm thickness and with 12.5 μm ^{7}Be window. More details are provided in the technical user manual. The energy resolution is 140 eV at 5.9 keV, which is about 2% value. The angle between the incident and emitted beam is 90° (with 45° optimization preference between the incident collimated x-rays and the normal to the sample's surface) as figure 3 shows real system's arrangement during acquisition. The geometry arrangement is the optimized measurement system so that the background noise due to Compton Scattering can be reduced. The positioning of the sample was set at the focal point of the two laser beams for

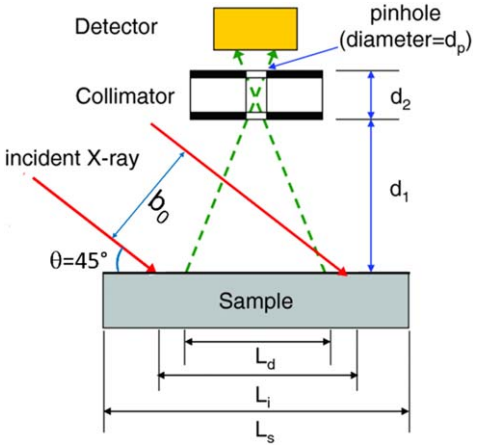

Figure 3. Representation of the system of detection used (x-ray incident beam and the geometry) for experiment with Silicon Drift Detector X-123SDD: θ varies in different measurement but in our experiment, $\theta = 45°$.

efficient irradiation and detection. Specification on the x-ray generator shows that it was operating on 50 kV and 50 μA of 900-seconds acquisition's time. Only experimental setup arrangements and conditions are set at the laboratory; the detector and software used are provided by another scientist (Solé *et al* 2007, Blagoev *et al* 2013, Smith *et al* 2015). This part of the study was performed directly on the surface of different pellets realized in the laboratory. Measurements were performed at three points of the sample surface and the considered result is the mean of the three in the case of very low deviation. The experimental setup used to perform our experiment was proposed and well described by Wenbin (Blagoev *et al* 2013, Smith *et al* 2015) and is represented in figure 3. Once acquired the XRF spectra, the PyMCA software package was used for data analysis and treatment.

2.3.2. Reference materials and PyMCA description

To check the precision and accuracy of the x-ray fluorescence spectrometry technic in the evaluation of major, minor and traces components in soil samples, GeoReM reference samples were used. A total of four (04) samples of reference were used for EDXRF calibration procedure. These samples were certified reference material (CRM) and were made and provided by the National Institute of Standards and Technology (NIST). It included NIST - SRM-610, PACS -2, MESS-3, and BE-N. These standard reference materials (SRMs) were produced and certified to facilitate the improvement of compound strategies for the analysis of elemental composition in geological samples. They were prepared in rod form and have been sliced into wafers in the laboratory. SRM-610 was used in a special way: it contains almost all the elements present in the sample. It is used to detect the presence of any element in the sample before refining its concentration with the other reference samples.

The configuration parameter of the acquisition system must be as straightforward as could be expected under the circumstances to fit the requirements. The setup used must have been validated there before. PyMCA (Python Multichannel Analyzer) was used as software for analyzing the obtained results. It is an application that relies on Python bindings bases on C++ Qt programming toolkit. It is necessary to highlight here that Qt is a C++ toolkit for cross-platform development (Van Espen *et al* 1977, Solé *et al* 2007, Kaniu *et al* 2012, Erick Towett *et al* 2013, Baba *et al* 2016). Background measurement was subtracted from the sample's experimental data prior to the least squares fitting and interpretation of the fluorescence peaks. PyMCA implements a fitting mode where the continuum is portrayed by an analytical function prior to the determination of different concentration (Van Espen *et al* 1977, Eivindsona and Mikkelsen 2001). Calibration curve for EDXRF analysis IS presented in figure 4 bellow and presented the range of energies of importance for elemental characterization.

The spectra (the calibration one and those from samples) were obtained with an equipment calibrated for acquisition of energy gap ranged from 0.12 to 30.5 keV covering the energy of Pb–L_α (10.552; 10.450), Pb–L_β (12.614; 12.623), Pb–L_γ (14.764); Th–L_α (12.969; 12.810), Th–L_β (16.202; 15.624), Th–L_γ (18.983); U–L_α (13.615; 13.439), U–L_β (17.220; 16.428), U–L_γ (20.167) and K–K_α (3.314; 3.311), K–K_β (3.590) where all fluorescence lines are expressed in keV (Nicholas and Zhang 1997).

The discriminant function of Roser and Korsch are also used for soils classification and provenance (Roser and Korsch, 1988). It uses major detected elements as variables. Provenance discrimination diagrams construct using major and trace element concentrations are very useful and certain appropriate ones are used for the provenance and tectonic assessment of sediment (Bhatia 1983, Taylor and McLennan 1985, Bhatia and Crook 1986). Some affecting factors are their moderately low mobility in sedimentary processes as well as their

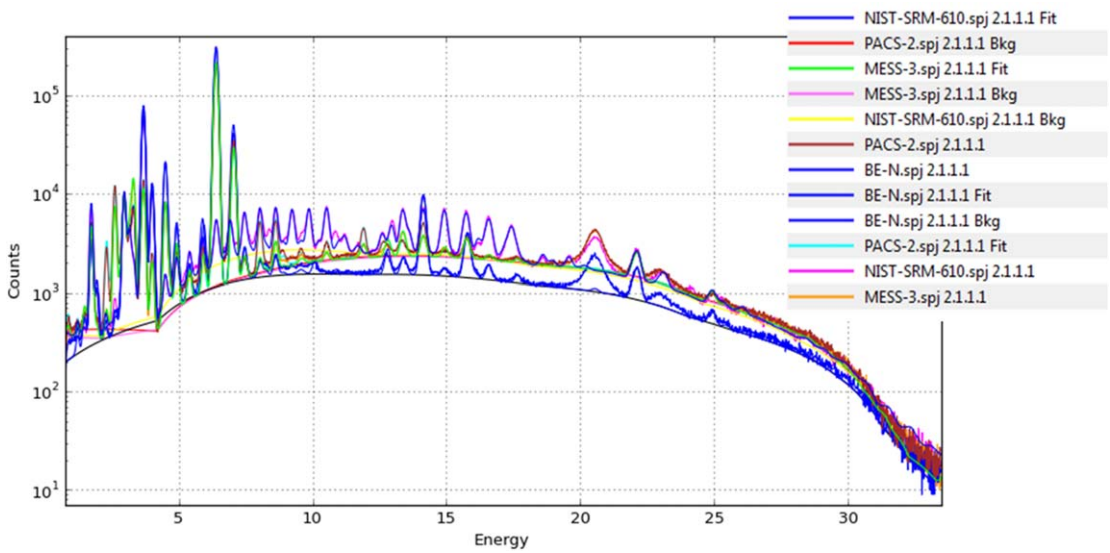

Figure 4. Calibration curve for EDXRF measurement: the four elements used in this process are NIST-SRM 610, PACS-2, MESS-3, and BE-N.

low residence time in seawater (high solubility and disintegration). Ti is very useful to assess this type of element for such geological provenance determination of studied samples. Diagrams were plotted using the major and minor elemental concentration as function and variables at the same time.

2.4. Gamma-ray spectrometry

Radiometric measurements were performed following the procedure of counting individual photons characterized by energy emitted from different radionuclides present in the investigated samples. Two analysis using fairly similar methods of detectors' calibration were performed with HPGe BE6530 model (to assess activity of two radionuclides: ^{226}Ra and ^{232}Th with low photon energy) and with GC0818-7600SL model (to assess ^{40}K radioactivity level which gamma-ray line is around 1460 keV higher than ^{226}Ra and ^{232}Th gamma-ray lines) (Guembou *et al* 2016). The 295.2 and 351.9 keV of ^{214}Pb and 1120.3 keV of ^{214}Bi γ-ray emission were used to monitor the activity concentration of ^{226}Ra. The case of ^{232}Th was resolved using the 911.2 and 969 keV ^{228}Ac γ-lines, while the 1460.8 keV gamma-ray line was used directly for ^{40}K with 95% confidence level uncertainties.

Guembou *et al* and many other authors presented the methodology used for radioactivity assessment in the present study (Guembou *et al*2016, 2017a, Tzortzis *et al* 2004). The sample analysis process was followed by the calculation of activity concentration in Bq/kg. Background subtraction was done on each sample' spectrum using Genie-2000 software v 3.2 and implemented algorithms accordingly (Genie 2000, Guembou *et al* 2016). This step included cascades summing correction as well as auto-absorption correction.

24 h were set as counting time for the acquisition of each sample and the spectral analysis was done using Genie 2000 software. The analyzing procedure included peak search, nuclide identification, activity and uncertainty calculation, MDA (for Minimum Detectable Activity) and including coincidence summing and self-absorption correction based on the following equation (Venkataraman *et al* 1999, Guembou *et al* 2016):

$$A(Bq/kg) = \frac{\frac{N_S}{t_S} - \frac{N_B}{t_B}}{M_S \times \varepsilon \times P_\gamma \times K_{SC} \times K_{SA} \times K_{DC}} \quad (1)$$

Where $A(Bq/kg)$, $\frac{N_S}{t_S}$, $\frac{N_B}{t_B}$, M_S, ε, P_γ, K_{SC}, K_{SA}, and K_{DC} referred to activity concentration of radionuclide, count rate for the sample, count rate for the background, sample's mass, efficiency, emission probability, cascade summing correction, correction factor for self- attenuation, and decay correction factor for radionuclide respectively (Venkataraman *et al* 1999, Mikael *et al* 2013, Guembou *et al* 2017b, Guembou *et al* 2016). uncertainties on the computed values using the previous formula are calculated with the formula presented by Guembou *et al* in 2018 (Guembou *et al* 2018, Hazou *et al* 2019).

To evaluate the radiation hazard connected with soils, the radium-equivalent activity (Ra_{eq}) was considered. This parameter evaluates the activity concentration in Bq/kg of a radionuclide equivalent to 370 of ^{226}Ra and gives outdoors the external effective dose rate of 1 mSv/year. The Ra_{eq} was defined in researches done by many authors (Guembou *et al* 2016, Ndontchueng *et al* 2014b, Beretka and Mathew 1985) and is based on the following relation:

$$Ra_{eq} = A_{Ra} + 1.43A_{Th} + 0.77A_K \quad (2)$$

Where A_i referred to the activity concentrations of the ith element and expressed in Bq kg^{-1}.

3. Results and discussion

Energy dispersive x-ray spectrometry analysis results for major, minor and trace elements' characterization are reported in tables 1, 2 and shown in figures 5–7.

3.1. Concentrations of major, minor and trace elements

Major and trace component investigation of eighteen (18) soil samples from the two campuses of Douala are recorded in tables 1 and 2. Table 1 shows the major element concentration of the soil samples. In *campus* 1, the most abundant elements found in all investigated soil samples are SiO_2 (mean value of 45.85%) and Fe_2O_3 (mean value of 17.79%). The presence of TiO_2, CaO, Al_2O_3, K_2O, and MnO (with mean concentration values of 10.10, 10.79, 5.11, 3.87 and 3.87 in term of percentage respectively) is also relevant. CaO is widely distributed in the Earth's crust with a mean concentration of 0.83% in this campus. The minor (trace) elements such as Na_2O and P_2O_5 were not detected in the major and minor analysis due to the setting of the detection limit during experiments.

From *campus* 2, the most abundant elements found in all investigated samples are also SiO_2 averaging 45.14% and Fe_2O_3 (mean value of 18.47%). The highest concentration of Fe_2O_3 was 22.26% found in sample UD9. The presence of TiO_2, CaO, Al_2O_3, K_2O, and MnO (with mean concentration values of 11.68, 9.31, 5.71, 2.95 and 4.11 in term of percentage respectively) is also relevant. The concentrations of MgO varied from 0.69 to 1.04% with a mean value of 0.86%. The concentration found in the majority of the investigated soil samples put into evidence that the analyzed sample can be classified as Fe-soil (or Fe-sand as presented by many other scientists) due to the concentration of Si and Fe in analyzed samples. This has been suggested after investigating the concentration of Fe in different soil samples. It is not very surprising that the concentration of Fe in samples is a little high compared to the same analysis in different countries. Many reasons may explain this high Fe concentration in the investigated samples, Douala Bassa area is the primary site for industrial activity in Cameroon as well as in Central Africa sub-region. In addition, the history of the campus shows that it was the valley of waste early the foundation of the city of Douala. The mineral composition of the parent rock (the primary geological formation) may be also one of the main reason for the high concentration of Fe.

Table 2 shows the trace elemental concentration of the soil samples. The most detected trace elements found in all investigated soils are S, Ca, Cr, Ni, Cu, Zn, Ga, As, Sr, Zr, Nb and Ag with mean concentration values of 240.0, 30.8, 5.3, 75.4, 23.6, 31.1, 2.4, 11.8, 3.1, 32.6, 2.0 and 21.7 μg/g for the samples from Campus 1 and 227.0, 26.6, 6.3, 76.0, 22.0, 26.2, 2.2, 11.6, 3.4, 29.9, 2.4 and 21.8 μg/g for the samples from Campus 2 respectively.

Tables 1 and 2 highlighted the differences in the elemental content found in investigated soil and these data can be included in the baseline data in Cameroon as well as in the sub-region of Central Africa. The soil' composition varies slightly from one sampling point to another. These differences are evidenced (or observed) in figure 5 and in tables 1 and 2, where the mean elemental content of all the elements obtained in eighteen analyzed soil samples is presented. It may be due to the non-uniform distribution of soil characteristics and geological and geochemical properties on the Earth. The agreement between obtained values of elemental concentration with literature are presented in different research studies (Baba *et al* 2016, Banas *et al* 2013, Erick Towett *et al* 2013, Franz *et al* 2013, Kaniu *et al* 2012, Kubala-Kukus *et al* 2015) and this was observed using PyMCA.

Figure 5 presents EDXRF spectra of soil samples from Campus 1, and similar spectra from Campus 2 were analyzed after acquisition simultaneously and presented in detail in the Annex section, figures A1, A2, and A3.

It can be also observed from the obtained result that the calibration procedure was well done because all elements' peaks are fixed at the same energy range (no translation of peaks can be observed) but just a difference in the count rate. For example, the concentration of Fe in different soil sample was concentrated into 14.78 to 22.26%. A slight variation can be observed (due to the background and difference found in different samples) and can be explained as the low statistical variation due measurement time and equipment and the history of the studied site previously explained. The observed variation probably suggests the different concentrations found in soil samples due to their age, their origin (geological materials which were included in their formation) and different past human activities. In this part, it is important to notice that the two studied sites were the discharging waste site of the urban community of Douala early its foundation. This discharging of waste also justified the higher level concentration of K_2O in the studied site comparing to other sites around the World (Baba *et al* 2016, Erick Towett *et al* 2013, Kaniu *et al* 2012, Kubala-Kukus *et al* 2015). It is necessary to fix background fluctuations in the case that the interest is about the peak determination and the related concentration values.

Low content of Cr, Ni, Cu, Zn, As, Sr, Zr, and Ag were found in the investigated samples, thus, does not exclude the possibility of environmental pollution. It shows the necessity of yearly assessment of radioactivity and heavy metal pollution. This can be done by measuring the elemental concentration of different elements

Table 1. Concentrations of major compounds and their standard deviation (s) in terms of percentage (%) of all soil samples from the two campuses.

Sample Point	SiO_2	s	Al_2O_3	s	K_2O	s	Fe_2O_3	s	TiO_2	s	MgO	s	CaO	s	MnO	s
UD1	48.55	0.24	5.21	0.09	6.99	0.12	17.04	0.02	7.84	0.03	0.80	0.03	9.64	0.11	2.17	0.44
UD2	48.76	0.11	7.26	0.11	3.51	0.10	21.08	0.02	12.56	0.04	0.98	0.03	1.82	0.08	2.07	0.60
UD3	44.53	0.09	4.83	0.08	4.99	0.11	15.87	0.01	8.35	0.03	0.74	0.02	14.98	0.12	3.87	0.43
UD4	51.92	0.10	4.43	0.08	3.13	0.10	17.68	0.02	5.56	0.02	0.83	0.02	12.06	0.11	2.64	0.42
UD5	45.66	0.09	4.68	0.08	2.52	0.09	17.00	0.02	10.84	0.03	0.79	0.02	11.03	0.10	5.61	0.41
UD6	40.57	0.09	4.21	0.08	2.65	0.10	18.25	0.02	13.21	0.03	0.85	0.02	12.09	0.11	6.54	0.45
UD7	40.93	0.09	5.14	0.09	3.28	0.11	17.64	0.02	12.34	0.03	0.82	0.03	13.94	0.12	4.20	0.47
Min	40.57	0.09	4.21	0.08	2.52	0.09	15.87	0.01	5.56	0.02	0.74	0.02	1.82	0.08	2.07	0.41
Max	51.92	0.24	7.26	0.11	6.99	0.12	21.08	0.02	13.21	0.04	0.98	0.03	14.98	0.12	6.54	0.60
Average	**45.85**	**0.12**	**5.11**	**0.09**	**3.87**	**0.10**	**17.79**	**0.02**	**10.10**	**0.03**	**0.83**	**0.03**	**10.79**	**0.11**	**3.87**	**0.46**
UD8	39.11	0.08	4.53	0.07	2.41	0.10	14.78	0.02	6.78	0.02	0.69	0.02	25.16	0.13	5.09	0.34
UD9	48.39	0.10	6.98	0.11	3.11	0.10	22.26	0.02	11.57	0.03	1.04	0.03	2.71	0.08	2.15	0.45
UD10	45.38	0.09	5.56	0.09	2.75	0.09	18.07	0.02	15.81	0.04	0.84	0.03	7.41	0.10	2.45	0.47
UD11	49.31	0.10	6.08	0.10	3.33	0.10	19.38	0.02	11.75	0.03	0.90	0.03	3.34	0.08	4.08	0.53
UD12	49.88	0.09	4.66	0.08	2.27	0.09	15.56	0.01	6.23	0.02	0.73	0.02	14.86	0.11	4.37	0.38
UD13	45.03	0.10	6.59	0.10	3.40	0.10	20.58	0.02	13.87	0.04	0.96	0.03	3.31	0.09	4.53	0.59
UD14	45.87	0.10	5.81	0.09	2.60	0.09	19.78	0.02	14.86	0.04	0.92	0.03	3.25	0.08	5.08	0.52
UD15	52.46	0.11	6.26	0.10	2.93	0.09	20.31	0.02	10.00	0.03	0.95	0.03	1.90	0.08	3.34	0.52
UD16	40.30	0.09	5.94	0.10	3.19	0.11	17.76	0.01	12.81	0.04	0.83	0.03	13.36	0.13	3.91	0.63
UD17	42.04	0.09	5.64	0.09	3.54	0.10	17.70	0.01	13.49	0.04	0.83	0.03	8.88	0.11	5.80	0.58
UD18	38.82	0.08	4.71	0.08	2.95	0.10	17.03	0.01	11.28	0.03	0.79	0.02	18.18	0.13	4.45	0.47
Min	38.82	0.08	4.53	0.07	2.27	0.09	14.78	0.01	6.23	0.02	0.69	0.02	1.90	0.08	2.15	0.34
Max	52.46	0.11	6.98	0.11	3.54	0.11	22.26	0.02	15.81	0.04	1.04	0.03	25.16	0.13	5.80	0.63
Average	**45.14**	**0.10**	**5.71**	**0.09**	**2.95**	**0.10**	**18.47**	**0.02**	**11.68**	**0.03**	**0.86**	**0.03**	**9.31**	**0.10**	**4.11**	**0.50**

Table 2. Concentrations of minor and trace elements and their standard deviation (s) in term of mg. g^{-1} (except only the case of S in μg. g^{-1} or ppm) of all soil samples from the two campuses. The detection limit for all the trace elements was set to be around 1 ppm except for the element S (~100 ppm).

Sample point	S	s	Ar	s	Ca	s	Cr	s	Ni	s	Cu	s	Zn	s	Ga	s	As	s	Sr	s	Zr	s	Nb	s	Ag	s
UD1	34	3	0.1	0.0	27.5	0.3	4.6	0.2	15.1	0.2	25.0	0.4	30.3	0.5	2.2	0.0	1.7	0.1	3.5	0.1	21.1	0.1	2.0	0.1	21.0	0.7
UD2	49	3	0.1	0.0	5.2	0.2	7.4	0.2	17.5	0.2	27.9	0.5	23.1	0.5	2.4	0.1	1.7	0.1	3.3	0.1	38.3	0.1	2.7	0.1	22.7	0.6
UD3	36	3	0.1	0.0	42.8	0.3	4.8	0.2	16.8	0.2	20.7	0.4	26.3	0.4	2.1	0.0	1.2	0.0	3.7	0.1	38.1	0.1	2.0	0.1	24.7	0.6
UD4	48	3	0.1	0.0	34.5	0.3	4.9	0.2	14.4	0.2	21.0	0.4	26.8	0.4	1.5	0.0	1.2	0.0	2.8	0.1	38.1	0.1	1.6	0.1	21.0	0.6
UD5	30	2	0.0	0.0	31.5	0.3	5.0	0.2	14.5	0.2	18.5	0.4	28.7	0.4	2.5	0.0	1.5	0.0	2.9	0.1	56.9	0.1	1.9	0.1	17.4	0.6
UD6	54	3	0.0	0.0	34.6	0.3	4.9	0.2	14.2	0.2	27.8	0.4	53.8	0.5	2.0	0.0	2.7	0.0	2.4	0.1	14.5	0.1	1.8	0.1	25.5	0.7
UD7	30	3	0.1	0.0	39.8	0.3	5.3	0.2	15.4	0.2	24.4	0.4	28.8	0.5	4.0	0.1	2.6	0.1	3.2	0.1	20.9	0.1	2.0	0.1	20.0	0.7
Min	30	2	0.0	0.0	5.2	0.2	4.6	0.2	14.2	0.2	18.5	0.4	23.1	0.4	1.5	0.0	1.2	0.0	2.4	0.1	14.5	0.1	1.6	0.1	17.4	0.6
Max	54	3	0.1	0.0	42.8	0.3	7.4	0.2	17.5	0.2	27.9	0.5	53.8	0.5	4.0	0.1	2.7	0.1	3.7	0.1	56.9	0.1	2.7	0.1	25.5	0.7
Average	**40**	**3**	**0.1**	**0.0**	**30.8**	**0.3**	**5.3**	**0.2**	**15.4**	**0.2**	**23.6**	**0.4**	**31.1**	**0.5**	**2.4**	**0.0**	**1.8**	**0.0**	**3.1**	**0.1**	**32.6**	**0.1**	**2.0**	**0.1**	**21.7**	**0.6**
UD8	12	2	0.0	0.0	71.9	0.4	3.3	0.1	13.8	0.1	15.8	0.3	25.1	0.4	2.2	0.0	1.8	0.0	2.9	0.1	13.9	0.1	2.0	0.1	16.9	0.6
UD9	42	3	0.1	0.0	7.7	0.2	5.2	0.2	17.1	0.2	32.5	0.5	22.0	0.5	2.3	0.1	1.6	0.1	3.1	0.1	29.9	0.1	3.1	0.1	29.9	0.7
UD10	13	3	0.1	0.0	21.2	0.3	7.5	0.2	18.2	0.2	27.5	0.4	33.0	0.5	3.6	0.1	1.5	0.0	2.6	0.1	28.2	0.1	3.0	0.1	21.0	0.6
UD11	33	3	0.1	0.0	9.5	0.2	7.1	0.2	17.8	0.2	26.5	0.5	27.4	0.5	2.2	0.1	1.6	0.1	3.5	0.1	35.7	0.1	2.3	0.1	22.2	0.6
UD12	22	2	0.1	0.0	42.4	0.3	4.0	0.2	16.4	0.2	23.4	0.4	22.0	0.4	1.9	0.0	1.6	0.0	2.8	0.1	14.8	0.1	1.8	0.1	20.2	0.6
UD13	37	3	0.1	0.0	9.5	0.2	7.6	0.2	12.5	0.2	21.2	0.5	15.1	0.5	1.7	0.1	1.5	0.1	3.5	0.1	19.7	0.1	2.4	0.1	24.4	0.7
UD14	34	3	0.1	0.0	9.3	0.2	6.1	0.2	13.9	0.2	16.6	0.4	20.2	0.5	1.8	0.0	1.6	0.1	3.0	0.1	41.8	0.1	2.4	0.1	21.4	0.6
UD15	41	3	0.1	0.0	5.4	0.2	7.1	0.2	17.9	0.2	25.4	0.5	19.0	0.5	2.3	0.1	1.3	0.1	3.3	0.1	42.3	0.1	2.2	0.1	21.4	0.6
UD16	16	3	0.1	0.0	38.2	0.4	8.4	0.2	15.3	0.2	16.0	0.4	25.2	0.5	2.6	0.1	1.6	0.1	5.2	0.1	19.1	0.1	2.5	0.1	21.7	0.7
UD17	22	3	0.1	0.0	25.4	0.3	6.4	0.2	17.5	0.2	20.6	0.5	44.1	0.5	2.0	0.0	1.7	0.1	3.6	0.1	51.5	0.1	2.5	0.1	21.1	0.7
UD18	26	3	0.1	0.0	51.9	0.4	6.1	0.2	15.7	0.2	17.0	0.4	35.3	0.5	1.7	0.0	2.0	0.0	3.6	0.1	31.7	0.1	1.8	0.1	19.4	0.6
Min	12	2	0.0	0.0	5.4	0.2	3.3	0.1	12.5	0.1	15.8	0.3	15.1	0.4	1.7	0.0	1.3	0.0	2.6	0.1	13.9	0.1	1.8	0.1	16.9	0.6
Max	42	3	0.1	0.0	71.9	0.4	8.4	0.2	18.2	0.2	32.5	0.5	44.1	0.5	3.6	0.1	2.0	0.1	5.2	0.1	51.5	0.1	3.1	0.1	29.9	0.7
Average	27	3	0.1	0.0	26.6	0.3	6.3	0.2	16.0	0.2	22.0	0.4	26.2	0.5	2.2	0.0	1.6	0.1	3.4	0.1	29.9	0.1	2.4	0.1	21.8	0.6

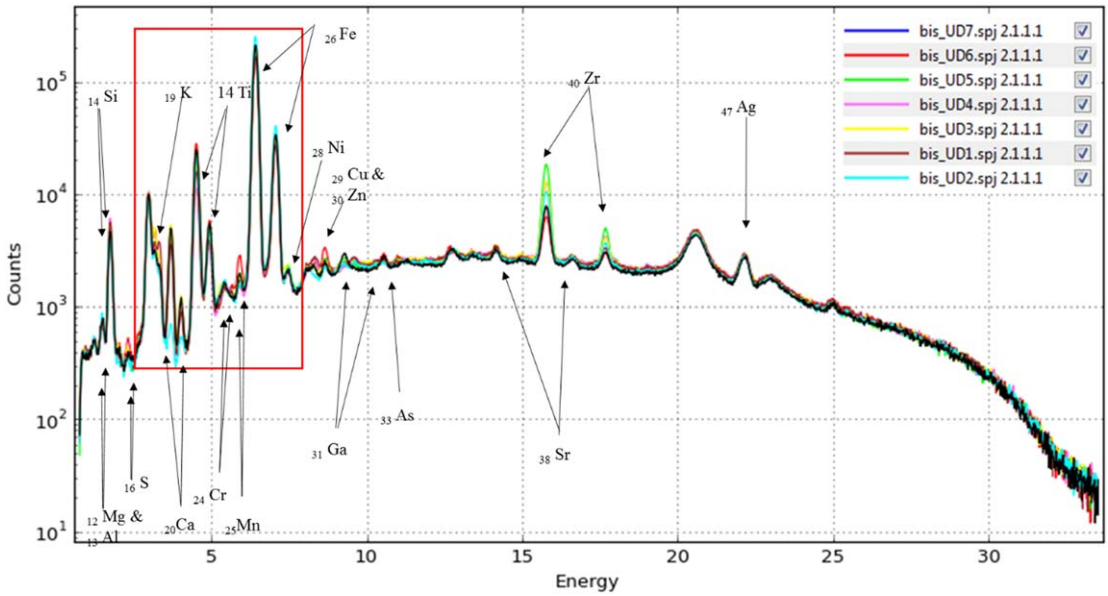

Figure 5. Spectra of different samples (UD1 to UD7) from Campus 1. All curves have similar composition and are represented on the same graph. A Comparative view of Fe and other surrounding representative peaks shown in the annex.

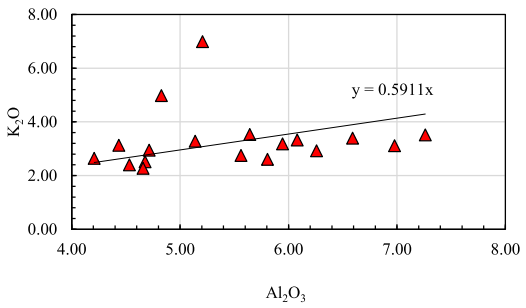

Figure 6. Positive correlation of K_2O and Al_2O_3.

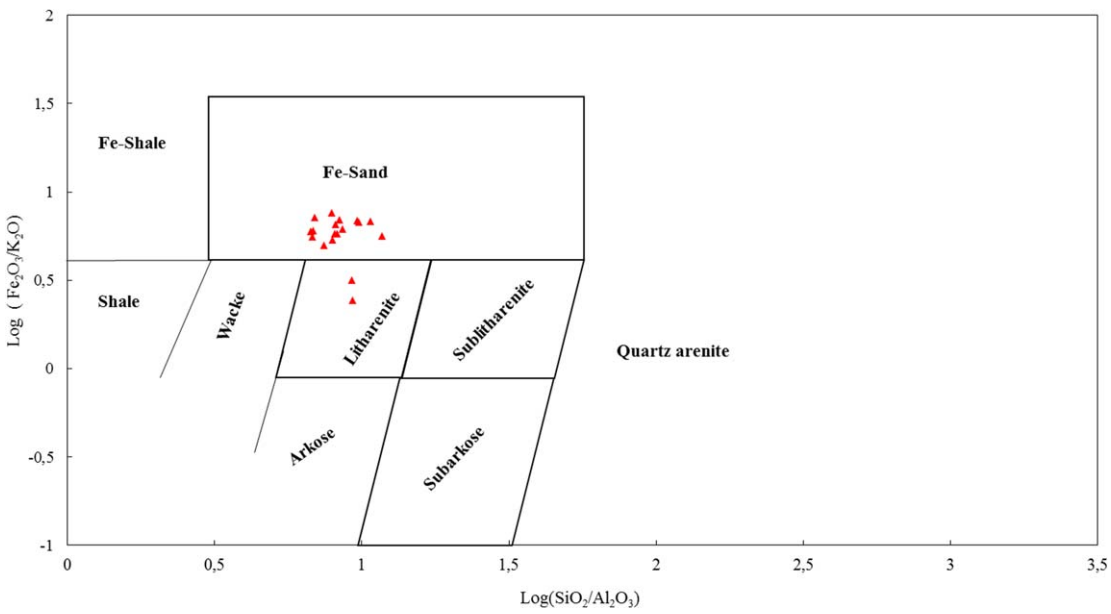

Figure 7. Chemical classification of the eighteen soil samples from Douala—Bassa area based on binary diagrams; log (SiO_2/Al_2O_3) as a function of log (Fe_2O_3/K_2O) diagram of Herron (Herron 1988).

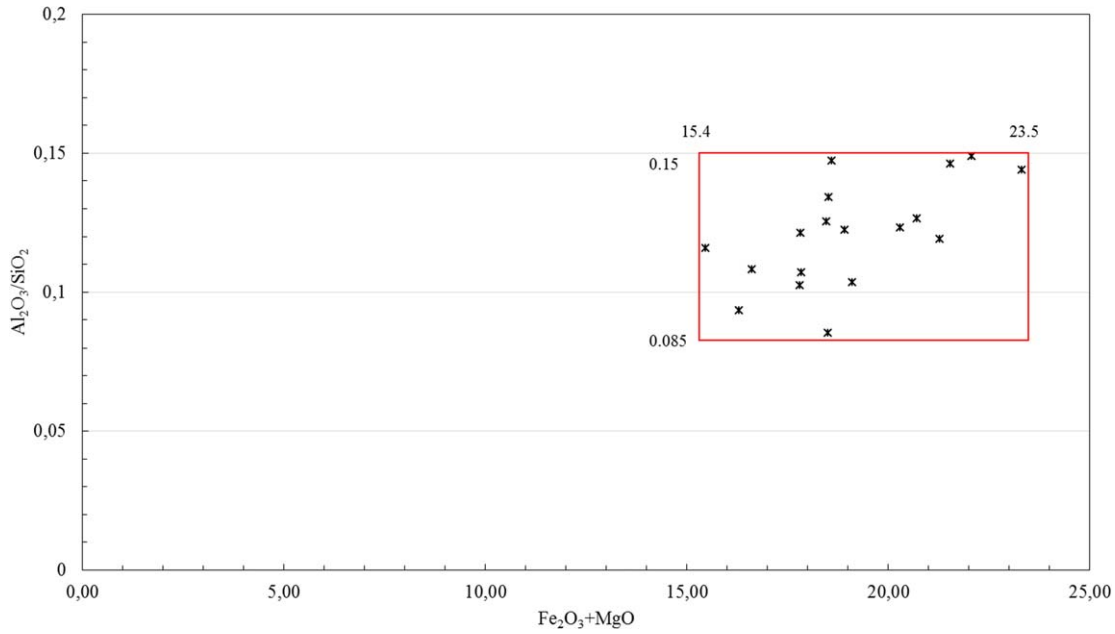

Figure 8. Al_2O_3/SiO_2 (%) as a function of Fe_2O_3 and MgO (%) for the different investigated soil samples (the discrimination diagram of tectonic for the determination of sediment provenance).

present in the studied site and correlated with the radioactivity concentrations. This study does not imply the correlation because the Pb (the main problematic heavy metal) concentrations in every sample were lower than the detection limit set for the acquisition.

3.2. Soil classification and provenance

3.2.1. Soil classification

As given in figure 6, the correlation between K_2O and Al_2O_3 concentrations, that is positive, infers that the K-bearing minerals have a noteworthy impact on the distributive existence of Al in the samples and highlights the relative abundance of these components in basic control set by the substance of mud mineral. Taking into account the Fe concentration in soil samples, it is found that the majority of the analyzed samples can be classified chemically as Fe-soil (Bhatia 1983, 1985a and Bhatia and Cook 1986). The discriminant functions (for the classification of the different type of soils) of Roser and Korsch (1988) used different variable oxide components as Al_2O_3, TiO_2, Fe_2O_3, MgO, CaO, Na_2O, and K_2O (Taylor and McLennan 1985). The use of this function was intended to present four different provenances of the sediments. The oceanic one so-called 'Mafic- ocean island arc', the solid continental one so-called 'Felsic - active continental margin', the middle of the previous two named 'Intermediate - mature island arc', and the last one, the 'Recycled –granitic, gneissic'. The comparison confirmed that all analyzed soils are illustrative dregs from the Continental margin (McLennan *et al* 1983, Roser and Korsch 1988). These results are further supported by low Al_2O_3/SiO_2 (as shown in figure 7) ratios that allowed the classification of less number of samples as being Litharenite (only two samples) and as Fe-sand or Fe-soil due to the higher concentration of Fe_2O_3 of the studied area (soil from other sixteen sampling points) (Chris *et al* 2013, Pettijohn *et al* 1987).

The classification of samples shown in figure 7 presents two groups of samples. The first characterization group so-called 'Fe-sand' by the literature is related to the important rate of Fe in samples. It shows that ~90% of investigated samples are classified as 'Fe-sand' or Fe-soil as the samples are soils. The second group containing two samples is Litharanite. Such information highlights the abundance of rock fragments in the investigated samples. Only around 10% of the sample are classified as Litharanite.

3.2.2. Provenance

Figure 8 reports Al_2O_3/SiO_2 (%) as a function of Fe_2O_3 and MgO (%) for the total eighteen samples analyzed from Douala and the so-called *diagram for the tectonic discrimination* which is provided here to discriminate the provenance of sediment formed by the samples (Bhatia 1985b, Fitton 1987). Description shows in figure 8 evidenced the Passive Margin origin of analyzed soil samples. Such results show that the process of alteration or erosion were not highly involved in the studied area during past centuries, but tectonic processes.

Different similar researches done in other areas in the World were examined to set the provenience of geological samples investigated in the present research. From the obtained results, it was observed that the samples from Douala basin presumably emerged from the dismantling, weathering, and transportation of raw materials present in the 'Gulf

Table 3. Specific activities of ^{226}Ra, ^{232}Th, and ^{40}K, and Ra_{eq} in investigated samples from Douala based on broad energy germanium detector (BEGe - Douala) and high purity germanium detectors' measurement GC0818-7600SL (Liege).

		Specific activity (Bq/kg)			
Sampling sites Laboratory of measurement	^{226}Ra Dla* (BEGe)	^{232}Th Dla (BEGe)	^{40}K Lge (7600SL)		Ra_{eq} Average
		26.70 ± 0.76	65.88 ± 1.55	117.94 ± 3.80	129.99
		28.95 ± 0.84	80.03 ± 1.87	195.72 ± 4.07	158.46
		21.99 ± 0.68	59.14 ± 1.41	218.30 ± 4.13	123.37
Campus 1		25.44 ± 0.77	63.27 ± 1.52	170.06 ± 3.94	129.01
		23.27 ± 0.71	59.78 ± 1.42	93.82 ± 3.74	115.98
		29.17 ± 0.87	71.06 ± 1.71	187.97 ± 4.10	145.26
		22.82 ± 0.69	62.57 ± 1.48	254.53 ± 4.27	131.89
Minimum		21.99 ± 0.68	59.14 ± 1.41	93.82 ± 3.74	115.98
Maximum		29.17 ± 0.87	65.88 ± 1.55	254.53 ± 4.27	158.46
Average values ± Standard Deviation		**25.48 ± 0.92**	**65.96 ± 7.39**	**176.91 ± 4.01**	**133.42**
		22.27 ± 0.68	52.60 ± 1.27	248.63 ± 4.28	116.63
		27.68 ± 0.80	62.79 ± 1.51	47.38 ± 3.60	121.12
		24.94 ± 0.73	72.50 ± 1.66	225.98 ± 4.65	146.02
		21.99 ± 0.68	63.93 ± 1.49	172.56 ± 4.21	126.65
		22.89 ± 0.69	64.46 ± 1.51	238.96 ± 4.63	133.47
Campus 2		25.87 ± 0.76	74.12 ± 1.71	225.65 ± 4.52	149.24
		23.84 ± 0.71	63.27 ± 1.48	198.16 ± 4.41	129.57
		26.74 ± 0.80	78.99 ± 1.83	260.74 ± 4.78	159.77
		24.64 ± 0.76	71.66 ± 1.69	244.97 ± 4.59	145.98
		24.98 ± 0.74	72.39 ± 1.66	240.18 ± 4.56	146.99
		23.67 ± 0.71	57.20 ± 1.36	271.76 ± 4.74	126.39
Minimum		21.99 ± 0.68	52.60 ± 1.27	47.38 ± 3.60	116.63
Maximum		27.68 ± 0.80	78.99 ± 1.83	271.76 ± 4.74	159.77
Average values ± Standard Deviation		**24.50 ± 1.80**	**66.72 ± 7.91**	**215.91 ± 4.45**	**136.53**
Worldwide	Range	17.00–60.00	11.00–68.00	140.00–850.00	
	Average	35.00	30.00	400.00	370

of Guinea' (Caldeira and Munha, 2002, Déruelle *et al* 2007, Gaudru and Tchouankoue, 2002, Halliday *et al* 1990, Marzoli *et al* 2001). The erosion actions in the past were one of the consequences of the geology observed nowadays in the study area as well as in many coastal areas and big basins in the World. Passive continental margins are found along the remaining coastlines. Since there is no collision or subduction occurring, tectonic activity is negligible and the Earth's weathering and erosional processes are winning. Sand and rock from Gulf of Guinea (the Rio Del Ray Basin) are acidic intrusive igneous (kind of rock containing about 20% of quartz), such as granites and metamorphic rocks such as gneiss. These results highlighted the presence of SiO_2 with high concentrations in analyzed soil samples. Information about weathering in a geological basin is also a subject matter of interest for petroleum industries (oil and gas resources are potential presents in such areas).

3.3. Activity concentration determination

The activity concentrations of natural radionuclides as ^{226}Ra, ^{232}Th and ^{40}K in analyzed soil samples are presented in table 3. Their values vary from one sampling point to another. The average activity concentration of ^{232}Th is higher than the worldwide usually assessed value recommended by UNSCEAR (2008). But, the activity concentration for ^{226}Ra and ^{40}K are lower than the world average value of 35 and 400 Bq kg^{-1} respectively (UNSCEAR 2008). The most abundant radionuclide is potassium. It is about 66% and 70% of the total (^{226}Ra + ^{232}Th + ^{40}K), ^{22}6Ra is 09% and 08%, and ^{232}Th is 25% and 22% in Campus 1 and Campus 2 respectively. Different values of the activity concentrations of ^{226}Ra, ^{232}Th, ^{40}K and radium equivalent activity in different soil samples are given in table 3.

As shown in table 3, the radioactivity measured in both studied sites slightly varied from one point to another. The gap between the minimum value and the maximum value for activity concentrations of ^{226}Ra, ^{232}Th, and ^{40}K is not as large as that observed in many other countries. This observed variation in radioactivity concentration of both studied sites may result from the non-uniform distribution of radionuclides and radioactivity contents present under the Earth crust (UNSCEAR 2008). The slight variation observed for both site may be due to the proximity of both sites. Considerable gab difference in Potassium-40 activity is also due to the irregular distribution of Uranium, Thorium (the two telluric radioactive series), and Potassium content in the investigated sites.

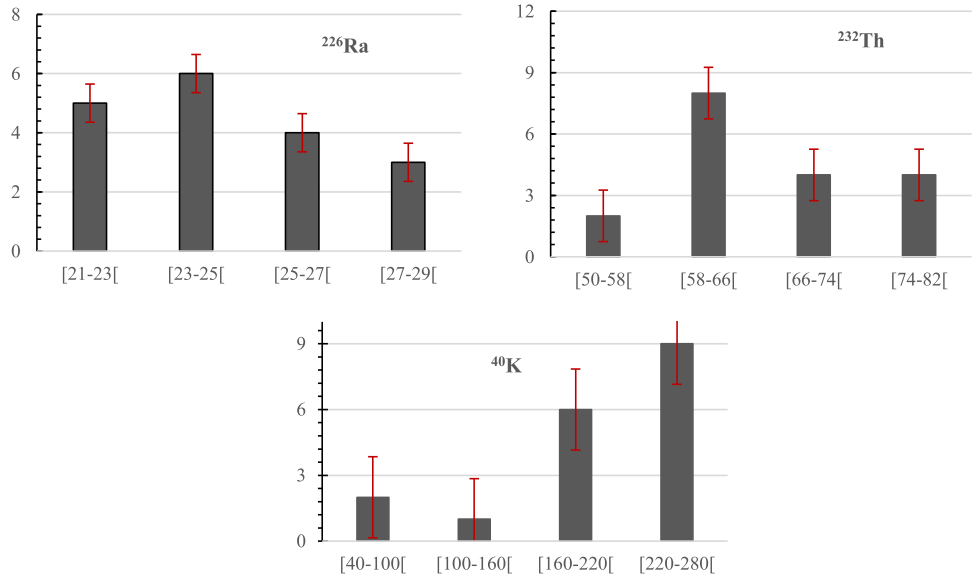

Figure 9. Diagram of frequency distributions of ^{40}K, ^{226}Ra and ^{232}Th in the analyzed soil samples (Douala–Cameroon).

3.3.1. Radium equivalent activity (Ra_{eq})

Ra_{eq} ranged from 115.98 to 158.48 with a mean value of 133.42 and from 116.63 to 159.77 with a mean value of 136.53 in campuses 1 and 2 respectively. The difference with the value of 370 is about 0.44 order of magnitude (mean $\sim 370^{0.44}$). These values are lower than the recommended worldwide value (UNSCEAR 2008, Guembou *et al* 2017a). The radiological analysis shows that these two campuses are safe as UNSCEAR and ICRP recommended values were not exceeded. The distribution of radionuclides in the analyzed samples shown a non-uniform trend in the terrestrial radioactivity variation in the study area.

3.3.2. Frequency distribution

Figure 9 shows the graph displaying the frequency distribution of the investigated samples. The description of ^{226}Ra, ^{232}Th, and ^{40}K activity concentrations in term of frequency shows fairly variation range of the radionuclides in the samples. 23–25 and 58–66 Bq kg^{-1} measured for ^{226}Ra and ^{232}Th, respectively (33% for ^{226}Ra and 44% for ^{232}Th) are the ranges that included most samples. This shows about half of the samples with ^{40}K activity concentration measures between 220 and 280 Bq kg^{-1}. Compare to the value of 30 Bq kg^{-1} (UNSCEAR 2008), the ^{232}Th's activity concentration showed a right translation and is higher in the majority of the analyzed samples (in all the investigated samples). Radium (Ra-226) and potassium (K-40) activity concentrations are lesser than the worldwide recommended values of 35 and 400 Bq kg^{-1} found in UNSCEAR report (2008) respectively. In conclusion, the radionuclide that most contribute to the radiological parameter in the area subjected to the present study is thorium (^{232}Th).

Average values of Ra_{eq} activity from both campuses are lower than the worldwide value of 370 Bq kg^{-1} measured by the United Nations Scientific Committee on the Effect of Atomic Radiation (UNSCEAR 2000). This value shows how the investigated area and people spending time in this area are less exposed to natural radiation, though are also subjected to less risk relies on the exposition to ionizing rays.

4. Conclusions

XRF analysis based on EDXRF method was performed for chemical characterization and all investigated soil samples were found to be illustrative dregs from Continental margin. Graph of correlation showed a positive gradient between the variation of K_2O and Al_2O_3. The plotted correlation (positive slope) then suggested a relative abundance of these components that are basically adjusted by the substance of mud minerals. This proved that analyzed samples in this study have the same origin and provenience (according to the obtained concentration values of Al_2O_3, TiO_2, Fe_2O_3, MgO, CaO, Na_2O, and K_2O).

Gamma-ray spectrometry measurements were also performed on the samples based on High Purity Germanium Detector. The gamma-ray spectrometry results present higher radioactivity of ^{232}Th of NORM than the global safe limits recommended by UNSCEAR (2008) but lesser in that of ^{226}Ra and ^{40}K. The radium equivalent values showed that the area of study is safe compared to the worldwide value of 370 Bk kg^{-1}

recommended by UNSCEAR. The observed activity concentration profile of the primordial radionuclides and the calculated radium equivalent activity show that no significant radiological risk can be observed. The obtained results of the two analytical techniques can be seen as baseline data for future investigations about elemental composition and radioactivity background levels in the study area. Measured activity concentrations confirm results obtained with the XRF analysis. The future project may consist on investigating the elemental characterization of the studied sited whether to correlate the natural radioactivity level with the presence of heavy metal or to determine if the pollution by heavy metal is due to industrial activity (time-dependent).

Acknowledgments

The authors are grateful to the **University of Porto** and **the University of Liege** and to the Professor Nathalie FAGEL (Department of Geology—University of Liege) for providing technical and financial support during experimentation and interpretation of data.

No conflict of interest.

Annex A : Spectra of different samples

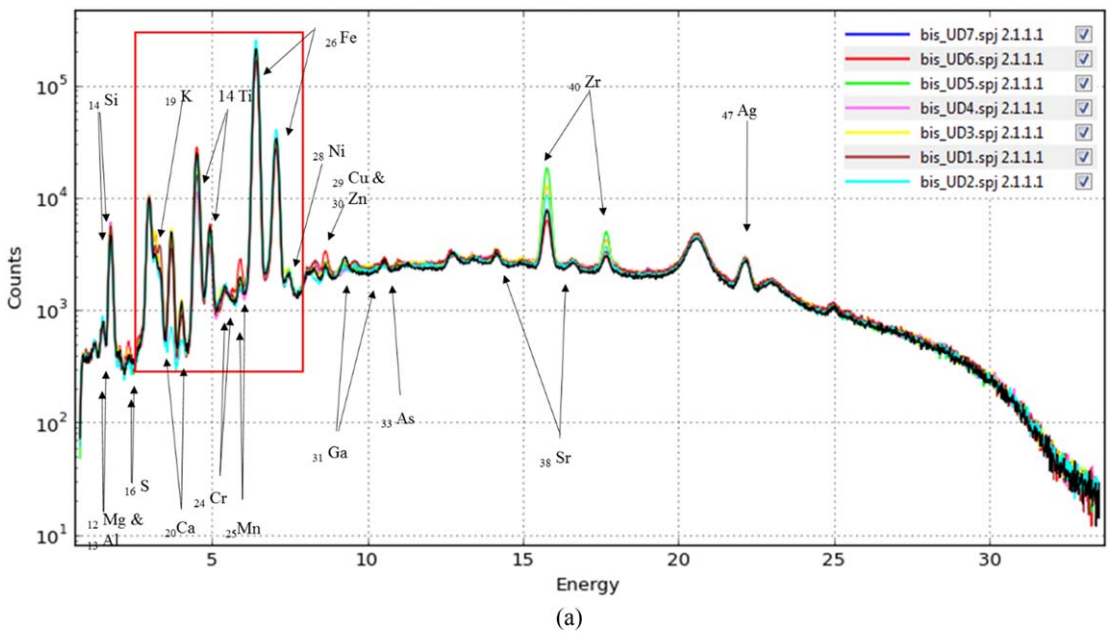

(a)

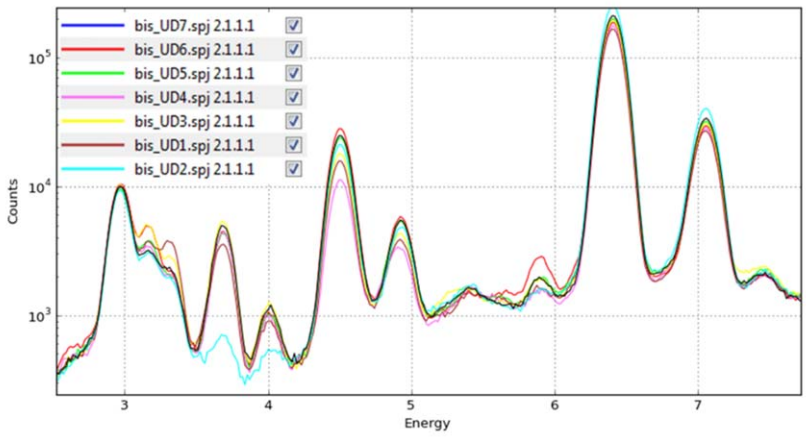

(b)

Figure A1. Spectra of different samples (UD1 to UD7) from Campus 1. (a) All curves have similar composition and are represented on the same graph. (b) A comparative view of Fe and other surrounding representative peaks.

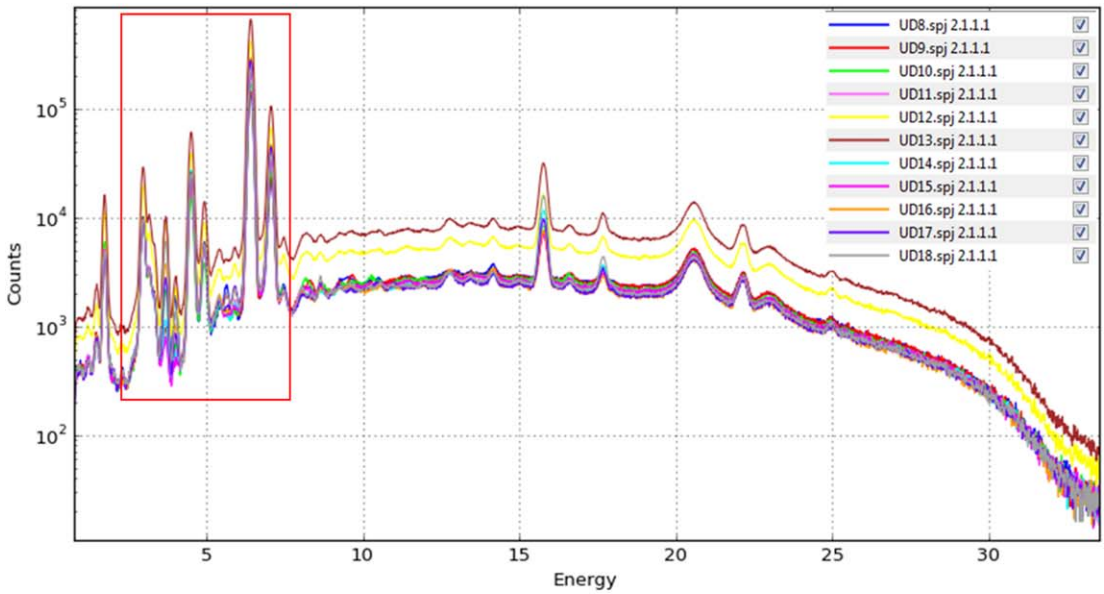

(a)

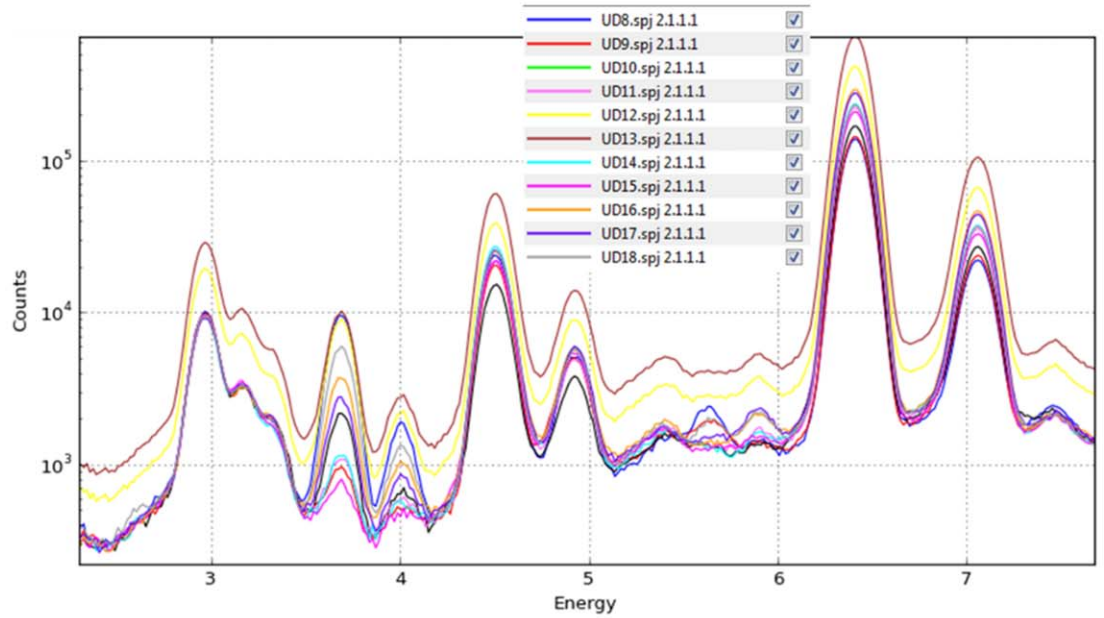

(b)

Figure A2. Spectra of different samples (UD8 to UD18) from campus 2. (a) All curves have similar composition and are presented in the same graph. (b) A comparative view of Fe and other surrounding representative peaks.

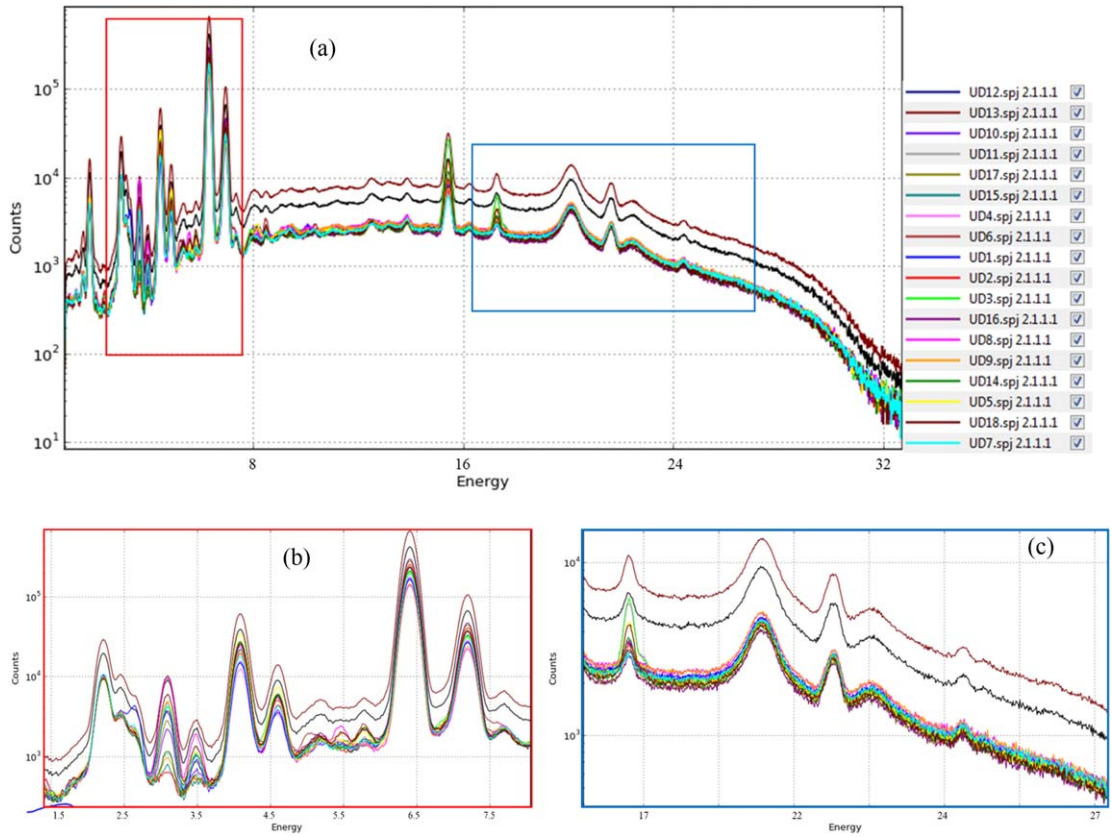

Figure A3. Spectra of different samples (UD1 to UD18) from campuses 1 and 2: (a) All curves have similar composition and are presented in the same graph. (b) A comparative view of the Ni, Sr, and Ag and other representative peaks (c) A comparative view of As, Zr, Sr, Kr, Rb, and other representative peaks.

ORCID iDs

Joel Cebastien Shouop Guembou https://orcid.org/0000-0003-4740-1146

References

Agarwal B K 1991 *X-Ray Spectroscopy* (Berlin Heidelberg: Springer)

Asaah Victor A, Akinlolu Abimbola F and Cheo Suh E 2006 Heavy metal concentrations and distribution in surface soils of the Bassa industrial zone 1, Douala, Cameroon *The Arabian Journal for Science and Engineering* **3** 147–58

Baba Y, Shimoyama I and Hirao N 2016 Chemical state analysis of trace-level alkali metals sorbed in micaceous oxide by total reflection x-ray photoelectron spectroscopy *Appl. Surf. Sci.* **384** 511–6

Banas D, Braziewicz J, Kubala-Kukus A, Majewska U, Pajek M, WudarczykMocko J, Czech K, Garnuszek M, Słomkiewicz P and Szczepanik B 2013 Study of absorption properties of chemically modified halloysite samples with x-ray fluorescence and x-ray powder diffraction methods *Radiat Phys Chem* **93** 129–34

Beretka J and Mathew P J 1985 Natural radioactivity of Australian building materials, industrial wastes and by-products *Health Phys.* **48** 87–95

Bhatia M R 1983 Plate tectonics and geochemical composition of sandstones *J. Geol.* **91** 611–27

Bhatia M R 1985a Plate tectonics and geochemical composition of sandstones: a reply *J Geol* **93** 85–7

Bhatia M R 1985b Rare earth element geochemistry of Australian Paleozoic graywackes and mudrocks: provenance and tectonic control *Sedimentary Geology* **45** 97–113

Bhatia M R and Crook K A W 1986 Trace element characteristics of graywackes and tectonic setting discrimination of sedimentary basins *Contributions to Mineralogy and Petrology* **92** 181–93

Blagoev K, Grozeva M, Malcheva G and Neykova S 2013 Investigation by laser-induced breakdown spectroscopy, x-ray fluorescence and x-ray powder diffraction of the chemical composition of white clay ceramic tiles from Veliki Preslav *Spectrochimica Acta Part* B **79** 39–43

Brjesson J and Mattsson S 2007 Medical applications of x-ray fluorescence for trace element research *Powder Diffr* **22** 130–7

Chris A, Moradeyo M, Atta-Peters D, Kutu J, Asiedu D and Boamah D 2013 Geochemistry and provenance of sandstones from Anyaboni and surrounding areas in the voltaian basin, Ghana *International Research Journal of Geology and Mining (2276-6618)* **3** 206–12

Caldeira R and Munha J M 2002 Petrology of ultramafic nodules from Sao Tome Island, Cameroon volcanic line (oceanic sector) *Jour. African Earth Sciences* **34** 231–46

Dziunikowski B 1989 Energy dispersive x-ray fluorescence analysis *Comprehensive analytical chemistry* **24** 431

Déruelle B, Ngounouno I and Demaiffe D 2007 The Cameroon hotline (CHL): a unique example of active alkaline intraplate structure in both oceanic and continental lithospheres *Comptes Rendus Géosciences* **339** 589–600
Eivindson T and Mikkelsen O 2001 Problems by using pressed powder pellets for XRF-analysis of ferrosilicon alloys *International Centre for Diffraction Data 2001. Advances in X-Ray Analysis* **44** 409–18
Erick Towett K, Keith Shepherd D and Georg Cadisch 2013 Quantification of total element concentrations in soils using total x-ray fluorescence spectroscopy (TXRF) *Sci Total Environ* **463** 374–88
Fitton J G 1987 The Cameroon line-West Africa: a comparison between oceanic and continental alkaline volcanism *Géol. Soc. Spec. Publ* **30** 273–91
Fittschen U and Falkenberg G 2011 Trends in environmental science using microscopic x-ray fluorescence *Spectrochim Acta* B **66** 567–80
Franz C, Makeschin F, Weib H and Lorz C 2013 Geochemical signature and properties of sediment sources and alluvial sediments within the Lago Paranoá catchment, Brasilia DF: a study on anthropogenic introduced chemical elements in an urban river basin *Sci Total Environ* **452–453** 411–20
Gaudru H and Tchouankoue J P 2002 The 1999 Eruption of Mt. Cameroon, West Africa *Co geo environment Newsletter* **18** 12–4
Genie 2000 *Operations Manual (2016) Part 1—The Genie 2000 Operations Manual, including the S501 Gamma Analysis option. Part 2 and 3—Model S505 QA Software User's Manual*
Glasby G P, Szefer P, Geldon J and Warzocha J 2004 Heavy-metal pollution of sediments from Szczecin Lagoon and the Gdansk Basin, Poland *Sci Total Environ* **330** 176–86
Guembou Shouop C J, Samafou P, Moyo Maurice N, Gregoire C, Nguelem Mekongtso E J, Ngwa Ebongue A, Motapon O and Strivay D 2016 Precision measurement of radioactivity in gamma-rays spectrometry using two HPGe detectors (BEGe-6530 and GC0818-7600SL models) comparison techniques: application to the soil measurement *Methods* X **4** 42–54
Guembou S C J, Moyo M N, Chene G, Mekongtso E J N, Motapon O and Strivay D 2017a Assessment of natural radioactivity and associated radiation hazards in sand building material used in Douala Littoral-Region of Cameroon, using gamma spectrometry *Environmental Earth Science* **76** 164
Guembou S C J, Samafou P, Ndontchueng M M, Chene G, Nguelem M E J, Takoukam S D, Werner V and Strivay D 2017b Optimal measurement counting time and statistics in gamma spectrometry analysis: the time balance *American Institute of Physics* **1792** 1–6
Guembou S C J, Moyo M N, Mekongtso E J N, Motapon O and Strivay D 2018 Monte Carlo method for Gamma spectrometry based on GEANT4 toolkit: efficiency calibration of BE6530 detector *J. Environ. Radioact.* **189** 109–19
Halliday A N, Davidson J P, Holden P, DeWolf C, Lee D C and Fitton J G 1990 Trace element fractionation in plumes and the origin of HIMU mantle beneath the Cameroon line *Nature* **347** 523–8
Hazou E, Guembou Shouop C J, Nguelem Mekongtso E J, Ndontchueng Moyo M, Beyala Ateba J F and Tchakpele P K 2019 Preliminary assessment of natural radioactivity and associated radiation hazards in a phosphate mining site in southern area of Togo *Radiat Detect Technol Methods (2019)* **3** 16
Hernández A J, Alexis S S and Pastor J 2007 Soil degradation in the tropical forests of the Dominican Republic's Pedernales province in relation to heavy metal contents *Sci Total Environ.* **378** 36–41
Herron M M 1988 Geochemical classification of terrigeneous sands and shales from core or log data *J. Sedimentary Petrol* **58** 820–829
Kaniu M I, Angeyo K H, Mwala A K and Mangala M J 2012 Direct rapid analysis of trace bioavailable soil macronutrients by chemometrics-assisted energy dispersive x-ray fluorescence and scattering spectrometry *Analytica Chimica Acta* **729** 21–5
Kheswa N Y, Papka P, Pineda-Vargas C A and Newman R T 2011 Target characterization by PIXE, alpha spectrometry and x-ray absorption *Nuclear Instruments and Methods in Physics Research* A **655** 85–7
Kubala-Kukus A *et al* 2015 X-ray spectrometry and x-ray microtomography techniques for soil and geological samples analysis *Nuclear Instruments and Methods in Physics Research* B **364** 85–92
Kubala-Kukus A, Ludwikowska-Kedzia M, Banas D, Braziewicz J, Majewska U, Pajek M and Wudarczyk-Mocko J 2013 Application of the x-ray fluorescence analysis and x-ray diffraction in geochemical studies of the Pleistocene tills from Holy Cross mountains *Radiat. Phys. Chem.* **93** 92–8
Manso M, Reis M A, Candeias J and Carvalho M L 2013 Portable energy dispersive x-ray fluorescence spectrometry and PIXE for elemental quantification of historical paper documents *Nuclear Instruments and Methods in Physics Research* B **298** 66–9
Marzoli A, Piccirillo E M, Renne P R, Bellieni G, Iacumin M, Nyobe J B and Tongwa A T 2001 The Cameroon volcanic line revisited: petrogenesis of continental basaltic magmas from lithospheric and asthenospheric mantle sources *J. Petrol* **41** 87–109
McLennan S M, Taylor S R and Eriksson K A 1983 Geochemistry of archaean shales from the Pilbara supergroup, Western Australia *Geochimica et Cosmochimica Acta* **47** 1211–22
Melquiades F L, Andreoni L F S and Thomaz E L 2013 Discrimination of land-use types in a catchment by energy dispersive x-ray fluorescence and principal component analysis *Appl. Radiat. Isot.* **77** 27–31
Melquiades F L and Santos F R 2014 Preliminary results: energy dispersive x-ray fluorescence and partial least square regression for organic matter determination in soil *Spectrosc. Lett.* **48** 286–9
Mikael H, Lutter G, Yüksel A, Marissens G, Misiaszek M and Rosengård U 2013 Comparison of background in underground HPGe-detectors in different lead shield configurations *Appl. Radiat. Isotopes.* **81** 103–8
Natara de Castilhos D B, Fábio Melquiades L, Edivaldo Thomaz L and Rodrigo Oliveira B 2015 X-ray fluorescence and gamma-ray spectrometry combined with multivariate analysis for topographic studies in agricultural soil *Appl. Radiat. Isotopes.* **95** 63–71
Navas A, Walling D E, Quine T, Machin J, Soto J, Domenech S and Lopéz-Vicente M 2007 Variability in ^{137}Cs inventories and potential climatic and lithological controls in central Ebro valley, Spain *J. Radioanal. Nucl. Chem.* **74** 331–9
Ndontchueng M M, Nguelem E J M, Njinga R L, Simo A and Guembou J C S 2014b Gamma emitting radionuclides in soils from selected areas in Douala-Bassa zone, littoral region of Cameroon *ISRN Spectroscopy* **2014** 1–8
Nicholas W E and Zhang W 1997 Millisecond X-Ray Pulsars in Low-mass X-Ray Binaries *The Astrophysical Journal* **490** 87–90 https://eur02.safelinks.protection.outlook.com/?url=https%3A%2F%2Fdoi.org%2F10.1086%2F311018&data=02%7C01%7Cmatthew.lang%40ioppublishing.org%7C8951d0d0fc4a46bf708308d6f65dbe71%7Cf9ee42e6bad04e639115f704f9ccceed%7C0%7C1%7C636967279821797505&sdata=7WDmt8oUXkfDIoX6JBF0fpBak4uvMpC1nZe6kLwzz4g%3D&reserved=0
Pettijohn F J, Potter P E and Siever R 1987 *Sand and Sandstone* 2nd edn (New York: Springer)
Radu T and Diamond D 2009 Comparison of soil pollutions determined using AAS and portable XRF techniques *Journal of Hazardous Materials* **171** 1168–71
Roser B P and Korsch R J 1988 Provenance signatures of sandstone mudstone suites determined using discriminant function analysis of major-element data' *Chemical Geology* **67** 119- 139
Smith A L, Colle J Y, Raison P E, Beneš O and Konings R J M 2015 Thermodynamic investigation of $Na_2U_2O_7$ using Knudsen effusion mass spectrometry and high-temperature x-ray diffraction *J. Chem. Thermodynamics* **90** 199–208

Solé V A, Papillon E, Cotte M, Walter P and Susini J 2007 A multiplatform code for the analysis of energy-dispersive x-ray fluorescence spectra *Spectrochimica Acta Part* B **62** 63–8

Stockmann U, Cattle S R, Minasny B and McBratney A B 2016 Utilizing portable x-ray fluorescence spectrometry for in field investigation of pedogenesis *Catena* **139** 220–31

Taylor S R and McLennan S M 1985 *The Continental Crust: Its Composition and Evolution* (Oxford: Blackwell Scientific) 312

Tsuji K, Injuk J and Van Grieken R E 2005 *X-Ray Spectrometry: Recent Technological Advances* (New York: Wiley)

Tzortzis M, Svoukis E and Tsetos H 2004 A comprehensive study of natural gamma radioactivity levels and associated dose rates from surface soils in Cyprus *Rad. Prot. Dos.* **109** 217–24

United Nations Scientific Committee on the Effect of Atomic Radiation (UNSCEAR) 2000 report to the general assembly*Annex B: Exposures from Natural Radiation Sources*

UNSCEAR 2008 *Sources and Effects of Ionizing Radiation, Report to the General Assembly with Scientific Annexes* Volume I, Annex B: Exposures from Natural Radiation Source United Nations, New York https://eur02.safelinks.protection.outlook.com/?url=https%3A%2F%2Fwww.unscear.org%2Fdocs%2Freports%2F2008%2F11-80076_Report_2008_Annex_D.pdf&data=02%7C01%7Cmatthew.lang%40ioppublishing.org%7C8951d0d0fc4a46bf708308d6f65dbe71%7Cf9ee42e6bad04e639115f704f9ccceed%7C0%7C1%7C636967279821797505&sdata=caezlHHk4Depk8TYIYdcW6RUFNQzIbzLfAhyjZi%2BDVA%3D&reserved=0

Van Espen P, Nullens H and Adams F 1977 A computer analysis of x-ray fluorescence spectra *Nucl. Instrum. Methods. Phys. Res.* B **145** 579

Van Grieken R and Markowicz A 1993 *Handbook of X-Ray Spectrometry* (New York: Marcel Dekker)

Venkataraman R, Bronson F, Abashkevich V, Young B M and Field M 1999 Validation of *in situ* object counting system (ISOCS) mathematical efficiency calibration software *Nucl. Instrum Methods Phys. Res. Sect A: Accelerat. Spectrom Detect. Assoc. Equip.* **422** 450–4

Walling D E 2013 The evolution of sediment source fingerprint investigations in fluvial systems *J Soils Sediments* **13** 1658–75

Wenbin L, Zhu J, Ma X, Li H, Wang H, Sawhney K J S and Wang Z 2012 Geometrical factor correction in grazing incident x-ray fluorescence experiment *Review of Scientific Instruments* **83** 1–5

Willis J P and Duncan A R 2008 *Understanding XRF Spectrometry* (Almelo: PANalytical B V)

World Weather Information Service (WWIS) 2016 Douala'*World Meteorological Organization* Retrieved 13 June 2016